# Intercomparison exercise on difficult to measure radionuclides in activated concrete - statistical analysis and comparison with activation calculations

Leskinen, Anumaija

2021-08

Leskinen , A , Gautier , C , Räty , A , Kekki , T , Laporte , E , Giuliani , M , Bubendorff , J , Laurila , J P , Kurhela , K O A , Fichet , P & Salminen-Paatero , S 2021 , ' Intercomparison exercise on difficult to measure radionuclides in activated concrete - statistical analysis and comparison with activation calculations ' , Journal of Radioanalytical and Nuclear Chemistry , vol. 329 , no. 2 , pp. 945-958 . https://doi.org/10.1007/s10967-021-07824-7

http://hdl.handle.net/10138/332992
https://doi.org/10.1007/s10967-021-07824-7

Journal of Radioanalytical and Nuclear Chemistry (2021) 329:945–958
https://doi.org/10.1007/s10967-021-07824-7

# Intercomparison exercise on difficult to measure radionuclides in activated concrete—statistical analysis and comparison with activation calculations

**Anumaija Leskinen[1] · Celine Gautier[2] · Antti Räty[1] · Tommi Kekki[1] · Elodie Laporte[2] · Margaux Giuliani[2] · Jacques Bubendorff[2] · Julia Laurila[3,4] · Kristian Kurhela[3,4] · Pascal Fichet[2] · Susanna Salminen-Paatero[3]**

Received: 4 April 2021 / Accepted: 4 June 2021 / Published online: 28 June 2021


## Abstract

This paper reports the results obtained in a Nordic Nuclear Safety Research project during the second intercomparison exercise for the determination of difficult to measure radionuclides in decommissioning waste. Eight laboratories participated by carrying out radiochemical analysis of $^{3}$H, $^{14}$C, $^{36}$Cl, $^{41}$Ca, $^{55}$Fe and $^{63}$Ni in an activated concrete. In addition, gamma emitters, namely $^{152}$Eu and $^{60}$Co, were analysed. The assigned values were derived from the submitted results according to ISO 13,528 standard and the performance assessments were determined using z scores. The measured results were compared with activation calculation result showing varying degree of comparability.

**Keywords** Difficult to measure radionuclides · Intercomparison exercise · Decommissioning waste · Concrete · Biological shield · ISO 13,528

## Introduction

A three-year intercomparison exercise project within Nordic Nuclear Safety Research (NKS) community on radiochemical analysis of difficult to measure (DTM) radionuclides in decommissioning waste began in 2019. The first year intercomparison exercise results on DTM analyses in an activated steel were published by Leskinen et al. [1, 2]. This paper presents the results of the second year intercomparison exercise, which was carried out on analysis of DTMs in an activated concrete. Similar to the first year, eight laboratories participated; three from Finland, one from Sweden, two from Norway, one from Denmark, and one from France. The focus was on determination of $^{3}$H, $^{14}$C, $^{55}$Fe and $^{63}$Ni whereas $^{36}$Cl and $^{41}$Ca were optional. In addition to DTMs, the key gamma emitters present in the activated concrete, namely $^{152}$Eu and $^{60}$Co, were measured. The results were analysed according to the ISO 13,528 standard [3], which enabled statistical analysis of the submitted results using robust methods. The samples were determined to be homogenous and the assigned values were derived from the submitted results according to the ISO 13,528 standard. The overall procedure was presented in the NKS report series [4] whereas in this paper, the results are further analysed and compared with activation calculation results. The studied activated concrete originated from FiR1 research reactor biological shield, for which the chemical composition, irradiation history and cooling time had been studied previously [5]. The calculated activity concentration results were derived using a combination of a MCNP neutron flux model [10] and a point kinetic code ORIGEN-S [6]. Preliminary activation calculation results on the DTM activity concentrations and chemical composition results were provided to the participants prior to the analysis phase. As such, low activity concentrations were expected. This paper discusses the final activation calculation results and compares them with the measured activity concentration results. Discussion on the

✉ Anumaija Leskinen
anumaija.leskinen@vtt.fi

[1] Technical Research Centre of Finland, Kivimiehentie 3, 02044 VTT Espoo, Finland

[2] Des-Service D'Etudes Analytiques Et de Reactivite Des Surfaces (SEARS), CEA, Université Paris-Saclay, F91191 Gif Sur Yvette, France

[3] Department of Chemistry, Radiochemistry, University of Helsinki, A.I. Virtasen aukio 1, P.O. Box 55, 00014 Helsinki, Finland

[4] Metropolia University of Applied Sciences, P.O. Box 4071, 00079 Metropolia, Helsinki, Finland

limit of detection (LOD) and uncertainty calculations among the participating laboratories are also presented.

## Sample history, homogeneity and stability

The studied activated concrete originated from the biological shield of 250 kW FiR1 TRIGA Mark II research reactor. FiR1 was the first nuclear reactor in Finland serving over 50 years in education, research, isotope production, and cancer treatment. The reactor was shut down permanently in 2015 and the dismantling is expected to begin in 2022. Characterisation of the FiR1 activated components has been carried out using both modelling and experimental studies [7–9]. Experimental characterisation of the biological shield began in 2014 with coring of inactive concrete cores to which, for example, testing of mechanical properties and chemical composition analyses were carried out. The results concluded that the concrete contained different types of stones mainly up to 32 mm, but also up to 80 mm diameter making the material quite heterogeneous in small scale. The chemical compositions of elements of interest determined in the inactive concrete core samples are presented in Table 1. The characterisation studies continued in 2018 when three activated concrete cores were taken from the activated part of the biological shield. The physical locations of the activated concrete cores were at different height and side of the biological shield compared to the inactive concrete cores. A separate article describing the calculation model and comparison between calculated and measured gamma activity concentrations in the cores as a function of distance from the irradiation source is under preparation by the corresponding affiliation. For this study, the most activated concrete core was sampled by drilling, which produced fine powder. The drilling procedure will be presented in an upcoming publication by the corresponding author. Due to the presence of different types and sizes of stones, a large sample size (approximately 180 g) was considered to produce a representative sample. Additionally, small grain size was expected to be easier for acid digestion due to a larger surface area. The drilled powder was mixed and 20 g was weighed into eight glass liquid scintillation vials. The homogeneity measurements were carried out according to the ISO 13,528 standard Sect. 6.1 "Homogeneity and stability of proficiency test items and Annex B" [3]. The homogeneity measurand was $^{152}$Eu activity concentration, because it was easy to measure as a gamma emitter and it had highest abundance in the samples. The measurements were carried out using a p-type HPGe semiconductor detector with 18% relative efficiency (ISOCS Canberra Ltd connected with Inspector 2000 multichannel analyser and Genie 2000 software). Geometry Composer v.4.4 was utilised for efficiency calibrations. The density of the drilled concrete, which is one of the parameters needed in the efficiency calculations, was calculated from the mass and volume of the samples. Each sample was carefully positioned on top of the detector in order to obtain a constant measurement geometry. The measurement time was 10,800 s. All samples were measured twice and the homogeneity was assessed using Eq. (1) as presented in the ISO 13,528 standard. The $s_s$ of the Eq. (1) was calculated from sample averages, between-test-portion ranges, general average, standard deviation of sample averages, within-sample deviation and between-sample standard deviation (equations presented in Annex B of the ISO 13,528 standard). However, because $\sigma_{pt}$ e.g. robust standard deviation of participant results was not known at the beginning of the project, relative standard deviation (RSD) of $^{152}$Eu results (average $19.7 \pm 0.3$ Bq g$^{-1}$) was estimated to represent homogeneity. As the RSD was 1.7%, the samples were considered homogenous. At the end of the project, when the $\sigma_{pt}$ was calculated from the submitted results, Eq. (1) was calculated to be true and therefore, the samples were homogenous also according to the ISO 13,528 standard.

**Table 1** Concentrations of elements of interest in three inactive concrete subsamples (internal data), activation reactions and thermal activation cross sections

| Element | Concentrations of three inactive concrete subsamples (mg kg$^{-1}$) | Activation reaction | Reaction thermal neutron cross section (barns) |
|---|---|---|---|
| Li | 36/27/39 | $^{6}$Li(n,α)$^{3}$H | $936 \pm 6$ |
| C | 1730/1835/2165 | $^{13}$C(n,γ)$^{14}$C | $(0.9 \pm 0.05) \times 10^{-3}$ |
| N | < 200 | $^{14}$N(n,p)$^{14}$C | $1.75 \pm 0.05$ |
| Cl | 55/56/59 | $^{35}$Cl(n, γ)$^{36}$Cl | $90 \pm 30$ |
| Ca | 91,000/79000/95000 | $^{40}$Ca(n, γ)$^{41}$Ca | $0.22 \pm 0.04$ |
| Fe | 23,000/21000/23000 | $^{54}$Fe(n, γ)$^{55}$Fe | $2.7 \pm 0.4$ |
| Ni | < 50 | $^{62}$Ni(n, γ)$^{63}$Ni | $15 \pm 2$ |
| Eu | 2.1/2.0/2.2 | $^{151}$Eu(n, γ)$^{152}$Eu | $5500 \pm 1500$ |
| | | $^{153}$Eu(n, γ)$^{154}$Eu | $1500 \pm 400$ |
| Co | 12/13/13 | $^{59}$Co(n, γ)$^{60}$Co | $20.2 \pm 1.9$ |

$$s_s \leq 0.3\sigma_{pt} \quad (1)$$

where, $s_s$ = between-sample standard deviation, $\sigma_{pt}$ = robust standard deviation of participant results.

The stability of the samples was considered in theoretical level based on the experience of the participants. The sample preparation, transport and storage were considered not to affect the stability of the samples, as they were solid materials and the DTMs were not volatile in normal storage and transport conditions. The only exception was $^{3}$H, which can be lost due to evaporation as tritiated water even at room temperature. Loss of $^{3}$H is especially problematic if it originates from contamination. In this study, $^{3}$H originated from activation and all loosely bound $^{3}$H was considered to have been released already during sampling. Evidence for $^{3}$H instability would have been possible to be carried out by comparing the submitted results with the measurement dates [3].

## Activation calculations

Estimating the activation reactions in the reactor structures was a two-stage process. First, a particle transport code was used to solve the neutron fluxes inside the reactor structures and components and then this data was used in a point-depletion code, which took the energy dependent neutron flux values from the transport calculations together with the material composition data and operating history to determine the quantity of neutron activation products. This study applied Monte Carlo based neutron transport code MCNP [10] and a point-depletion code ORIGEN-S [6]. The procedure utilised is presented in Fig. 1 [11].

The activation calculations modelled the whole operating history of the FiR1 research reactor throughout the years 1962–2015 as described in Ref. [11]. Major structural changes during the reactor operating history were taken into account by creating different neutron transport models for different phases of the operating history and combining all of these in the point-kinetic calculation. Altogether three separate time periods were modelled.

The biological shield concrete core was drilled close to a horizontal neutron beam tube. The beam tube had been plugged in the late 1980's. However, it was impossible to model the details of all the experiments and research devices used inside the beam tube in the 1960's and 1970's. Therefore, the calculation model assumed conservatively that the beam tube had been empty before the plugging, whereas in reality, several different types of research equipment with unknown time intervals had been placed inside the beam ports causing unknown amounts of neutron absorption and scattering. This assumption overestimated the neutron fluxes around the beam tube, but was considered acceptable for conservative initial calculations in estimation of total waste volumes. The calculation results were used in this article by assuming that the concrete nuclide vector (relative nuclide-wise activities) was correct and the results were scaled using the measured gamma-activities from the key nuclide $^{152}$Eu.

Although the neutron flux was estimated conservatively, the chemical composition of the concrete used in the calculation model was determined from three inactive cores that had been drilled earlier from the inactive outer parts of the reactor structure as described earlier [7]. The samples were

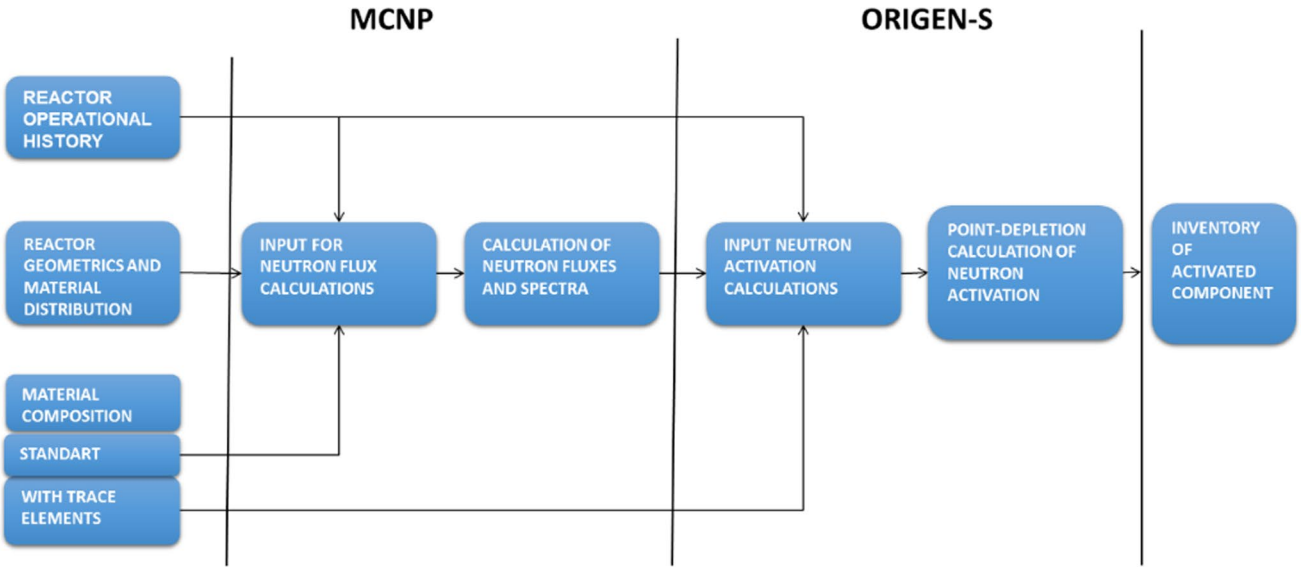


**Fig. 1** Overview of the applied calculation steps [11]

homogenised and their compositions were measured separately using CHN pyrolyser (C, H and N), AOX pyrolyser (Cl), ICP-MS (B, Ba, Co, Cs, Eu, Li, Ni, Sm and U), and ICP-OES techniques (Al, Ca, Fe, K, Mg, Mn, P, S, Si and Ti). For conservatism, the highest measured concentration (or LOD) of each activating element was used in the calculation model. The concentration results of the relevant stable elements for this study in the three core samples are shown in Table 1. Point-depletion code ORIGEN-S uses built-in ENDF/B-VI formatted cross sections, but for illustration, Table 1 also lists the activation reactions and reaction cross sections according to Ref. [12].

## Methodology for statistical analysis

Statistical analysis of the submitted results was carried out using the ISO 13,528 standard on proficiency testing by interlaboratory comparison [3]. One major drawback of the ISO 13,528 standard is the lack of uncertainty considerations of the submitted results. However, due to consistency, the ISO 13,528 standard was utilised similar to the first year [2]. As the studied activated concrete was not a reference material, the assigned values were calculated using the submitted results. Robust means and robust standard deviations were calculated using Algorithm A, which is robust for outliers. The iterations of the robust mean and standard deviations were continued until there was no change in their third significant figure [3]. The robust means and standard deviations calculated from the participant's results are referred to as measured assigned values. The submitted results were also compared with calculated assigned values, which were determined based on the activation reactions.

Performance assessment was carried out using z score of Eq. (2), which was a recommended method in cases when the assigned value is calculated from the submitted results [3]. The submitted results (noted $x_i$) were assessed against both measured assigned values and calculated assigned values. In cases, when the robust standard deviation was large e.g. over 20%, the uncertainty of the assigned value $u(x_{pt})$ calculated using Eq. (3) was used as $\sigma_{pt}$ [3]. Selection of the $u(x_{pt})$ as $\sigma_{pt}$ was the prerogative of the intercomparison exercise organiser in order to produce fit for purpose assessments [3]. The z score results were acceptable when $|z| \leq 2.0$, a warning signal was given for results with $2.0 < |z| < 3.0$, and $|z| \geq 3.0$ results were unacceptable [3].

$$z_i = \left(x_i - x_{pt}\right)/\sigma_{pt} \quad (2)$$

where, $x_i$ = the value given by a participant i, $x_{pt}$ = the assigned value, $\sigma_{pt}$ = standard deviation for the proficiency assessment

$$u\left(x_{pt}\right) = 1.25 \times s^*/p^{0.5} \quad (3)$$

where, s* = robust standard deviation of the results, p = number of samples.

## Overview of the radiochemical analyses

The radiochemical methods utilised in the DTM analysis of the activated concrete have been summarised by Leskinen et al. [4]. The utilised procedures were mainly based on published references [13–27], but also internal procedures and modifications based on discussions between the participating laboratories. The main focus was given for $^{3}H$, $^{14}C$, $^{55}Fe$ and $^{63}Ni$ whereas $^{36}Cl$ and $^{41}Ca$ were optional. In general, the applied methods were divided between the volatile (e.g. $^{3}H$, $^{14}C$ and $^{36}Cl$) and non-volatile (e.g. $^{41}Ca$, $^{55}Fe$ and $^{63}Ni$) DTMs. The volatile DTMs were mainly analysed using thermal oxidation using a Pyrolyser (RADDEC) or an Oxidiser (Perkin Elmer) system. In thermal oxidation systems, volatile DTMs were trapped in different trapping solutions e.g. $^{3}H$ in 0.1 M $HNO_3$ solution, $^{14}C$ in CarboSorb or CarbonTrap solutions, and $^{36}Cl$ in 6 mM $Na_2CO_3$ solution. The $^{3}H$ and $^{14}C$ solutions were directly analysed in the trapping solutions using Liquid Scintillation Counting (LSC) whereas $^{36}Cl$ solutions required further purifications using AgCl precipitation and anion exchange resin prior to the LSC measurements. One laboratory also carried out the $^{14}C$ and $^{36}Cl$ analysis using a closed system on a heating mantle.

Even though the solubility of activated concrete was a major challenge and alkali fusion may have been a better method of choice, all the participants utilised acid digestion method for the destruction of the solid matrix in the analysis of non-volatile DTMs. Both acid digestions on heating mantles, hotplates and microwave ovens were utilised with strong acids i.e. mixtures of HCl, $HNO_3$, HF, $HClO_4$. The successfulness of acid digestions is discussed in the results section. After the acid digestions, mainly hydroxide precipitations with NaOH or $NH_4OH$ were implemented in order to separate Fe and Ni from Cs, Sr, Ba, Ra and namely Ca, if analysed. This precipitation was recommended during project discussion to be carried out very carefully with saturated NaOH up to pH 1 and then with mild NaOH (< 0.5 M) to pH 8–9. Use of mild NaOH was proposed to prohibit precipitation of Ca in lower pH range resulting either in lower Ca yields in Ca fraction or Ca interference in Fe and Ni separations. Fe and Ni were separated from each other and from cobalt using an anion exchange resin. However, one laboratory precipitated and removed AgCl prior to Fe and Ni separation using TRU resin and another laboratory carried out anion exchange resin separation of Fe and Ni without hydroxide precipitation. Purified Fe fractions were evaporated to dryness and

the residue was dissolved into 0.5 M $HNO_3$ or 1 M/3 M $H_3PO_4$, the latter acid has been discussed to cause the least amount of color quenching in LSC measurements [2, 27]. Ni fractions after the anion exchange resin treatment were further purified with Ni resin (Eichrom Technologies) once or twice. The purified Ni fractions were evaporated to lower volumes prior to LSC measurements.

Two laboratories based their analyses of $^{41}Ca$ on sequential precipitations of Ca as carbonates and hydroxides. Precipitations were carried out with and without heating and the precipitates and supernatants were separated using centrifugations. Contrary to referenced procedures in which the final hydroxide precipitate was dissolved in 4 M HCl and pH of the solution raised to pH 6–7 [19] or dissolved in 0.1 M HCl [17], the precipitate was recommended to be dissolved into conc. HCl and evaporated to dryness in order to produce water soluble $CaCl_2$. The $CaCl_2$ precipitate was dissolved in small amount of deionised water (3–4 ml) prior to the LSC measurements.

One laboratory purified Ca-containing solution, separated from Fe and Ni by their hydroxide precipitation, with oxalate precipitation of Ca from the solution and two different anion exchange steps. Ca oxalate precipitation was calcined at 600 °C over night and dissolved to 8 M HCl prior to first anion exchange separation. Ca was eluted in 8 M HCl, evaporated and dissolved to 8 M $HNO_3$ for the second anion exchange separation. Ca was eluted in 8 M $HNO_3$ and the acid fraction was evaporated to dryness. The residue was dissolved in 3–4 ml of 0.1 M HCl and measurements of stable Ca by MP-AES (Microwave Plasma—Atomic Emission Spectrometer) and $^{41}Ca$ by LSC were followed.

The LSC measurements of all DTMs (i.e. volatile and non-volatile) were carried out by mixing aliquots of the purified fractions with liquid scintillation cocktails (mainly Ultima Gold, but also Optiphase HiSafe 3) prior to the LSC measurements using counters such as Quantulus 1220 LSC, HIDEX 300SL, and AccuFLEX LSC-8000. The measurement efficiencies were determined using standard solutions for quenching corrections or TDCR (Triple-to-Double Coincidence Ratio) technique [28].

The $^{3}H$ and $^{14}C$ yields were determined using experimental estimations based on behaviour of liquid standards. $^{36}Cl$, $^{41}Ca$, $^{55}Fe$ and $^{63}Ni$ yields were determined using UV–Vis, ICP-OES, ICP-MS, MP-AES or standard addition. In one case, Fe yield was estimated to be 90% based on the in-house experience. The yields are further discussed in results section as the solubility of the matrix was not always complete and the concrete contained significant amounts of stable Fe, which was not always diligently considered in yield corrections.

## Overview of the gamma spectrometric analyses

All the laboratories carried out analysis of $^{152}Eu$ and $^{60}Co$ in solid form. Some laboratories also carried out gamma analysis of dissolved samples but the results suffered from low activities due to low sample sizes. The geometries of the solid sample measurements were glass/plastic vials and a petri dish. The samples were placed on top of high purity germanium (HPGe) detectors, which all participants utilised. Variety of efficiency calibrations were used, namely calibration solutions with LVis (Gamma vision) with EFFTRAN coincidence correction, ISOCS or LabSOCS (Mirion Technologies) and dual polynomial fitting. One laboratory carried out efficiency corrections based on experience due to lack of efficiency calibration for the LSC vial geometry. One laboratory prepared in-house concretes spiked with gamma emitters to establish an efficiency calibration specific for concretes.

## DTM and gamma emitter results and statistical analysis

The complete destruction of the solid matrix was challenged by the low solubility of concrete even in strong acids. Even though majority of the laboratories reported up to 100% dissolution with exception of proposed silica residues, in some cases the completeness of the acid digestions was estimated to be as low as 60% (Table 2). Additionally, it was not completely clear how some laboratories took into consideration the original amounts of Ca, Fe and Ni in the activated concrete, because only three laboratories carried out the chemical composition analysis of the acid digested solutions. Especially large amount of Fe caused significant problems in the ion exchange resin separations and result calculations as discussed later. Large amount of stable Ca did not affect the results as much as Fe, since Ca was analysed only by a couple of laboratories and majority of them analysed its content in the acid digested solution. Stable Ni content was low compared to the amount of added Ni carrier (0.05–4 mg) and therefore, its original content did not affect the results. Comparison of Tables 1 and 2 show that on average, the participant's Ca concentration results were 58–81% of the concentrations used in the activation calculations, Fe results were 82–95% whereas Ni results were below or close to detection limit and therefore not applicable. One reason for the difference may be, that the dissolution of Fe and larger fraction of Ca has not been complete with the selected methods of three reported laboratories. Additionally, the

**Table 2** Stable Ca, Fe and Ni concentrations in the activated concrete based on acid digestion results

| ID # | Estimated completeness of acid digestion (%) | Ca (mg/g) ± 2σ | Fe (mg/g) ± 2σ | Ni (mg/g) ± 2σ |
|---|---|---|---|---|
| 1 | 100 | – | – | – |
| 2 | < 100, silica residue | – | – | – |
| 3 | 100 | – | – | – |
| 4 | 85 | 51 ± 10 | 21 ± 4* | 0.020 ± 0.006 |
| 5 | – | – | – | – |
| 6 | 100, silica residue | 71 ± 10 | 19 ± 3 | < LOD |
| 7 | 60 | 54 ± 8 | 18 ± 2 | < LOD |
| 8 | 100, silica residue | – | – | – |

*Estimated from Ni yield during the leaching step (the loss of stable Fe for the leaching step was assumed to be the same as for stable Ni carrier, i.e. 70%)

data in Table 1 was measured from another FiR1 core sample, which was on a different height of the biological shield, which may have contained different types of stones. However, it is unfortunate that elemental concentration data is not available from all participating laboratories, especially from the ones that reported complete dissolution of the concrete material.

In total, 13 $^{55}$Fe and $^{63}$Ni results were submitted and the entries with sample numbers, sample sizes, yields and activity concentrations are presented in Table 3. The results show that 7 out of 13 $^{55}$Fe entries were above limit of detection (LOD) and minimum amount of sample to produce activity concentration results above LOD was 3 g. However, the results varied significantly from 0.1 to 8.1 Bq g$^{-1}$. The large variation was estimated to originate from a combination of the following parameters i) varying completeness of the acid digestions affecting the activity concentration calculations, ii) the high original stable Fe content, which was not always analysed or taken into consideration, iii) possible interference caused by luminescence, quenching and spectral interferences, and iv) low activity. Since the $^{55}$Fe activity concentration results varied significantly, the statistical analysis was not possible. Additionally, the yields for $^{55}$Fe varied significantly from 13 to 101%. However, not enough information on the yield calculations (i.e. how original Fe in the concrete was considered) was submitted.

$^{63}$Ni results in Table 3 show that only 3 out of 13 results were above LOD and minimum amount of sample to produce measurable activity concentrations was 5 g. The purified $^{63}$Ni fraction of sample number 7 with 10 g of

**Table 3** Measured $^{55}$Fe and $^{63}$Ni activity concentrations and corresponding masses, yields and z-scores compared to measured assigned value, if applicable

| ID # | Mass (g) | $^{55}$Fe results | | $^{63}$Ni results | | |
|---|---|---|---|---|---|---|
| | | Yield (%) | Activity concentration (mBq g$^{-1}$) | Yield (%) | Activity concentration (mBq g$^{-1}$) | z-score meas |
| 1 | 3 | 90 | 370 ± 20 | 24 | < 100 | |
| 1 | 3 | 95 | 340 ± 20 | 83 | < 100 | |
| 1 | 3.5 | 101 | 350 ± 20 | 90 | < 100 | |
| 2 | 10 | 64 | 1590 ± 940 | 24 | 700 ± 160 | 1.4 |
| 3 | 5 | 90* | 8100 ± 200 | 99 | 1100 ± 200 | 0.7 |
| 4 | 5 | 58*** | < 340 | 30 | < 310 | |
| 5 | 10 | ** | 110 ± 40 | ** | 1120 ± 150 | 0.8 |
| 6 | 0.6 | 13 | < 500 | 114 | < 600 | |
| 6 | 0.6 | 18 | < 400 | 102 | < 600 | |
| 6 | 0.6 | 19 | < 400 | 101 | < 600 | |
| 7 | 10 | 57 | 2600 ± 4100 | 77 | < 450 | |
| 8 | 0.5 | 32 | < 500 | 87 | < 90 | |
| 8 | 0.5 | 53 | < 300 | 85 | < 90 | |

*Estimated

**Data not submitted

***The loss of stable Fe for the leaching step was assumed to be the same as for stable Ni carrier (around 70%)

concrete suffered from burning of DMG precipitate causing significant colour quenching. Even though 3 entries were not considered to be a sufficient amount of data entries for reliable statistical analysis, 10 iterations with Algorithm A were carried out in order to produce fit for purpose $^{63}$Ni assigned value, namely 970 ± 380 mBq g$^{-1}$ (2σ). As the robust standard deviation of the assigned value was above 20% (i.e. 27%), standard uncertainty of the assigned value was utilised in the z score calculations. As such, all the $^{63}$Ni data entries above LOD were in acceptable z score range. On the other hand, some of the submitted LOD values are significantly below the assigned value, especially for samples 1 and 8. Critical considerations in LOD calculations are discussed later whereas here the results show clearly that LOD calculations need to be carried out carefully. The yield for $^{63}$Ni was 24–114%, varying similarly with the corresponding values for $^{55}$Fe. One participant, which did not carry out Ca analysis (i.e. no separation of Ca from Ni and Fe) reported difficulties in Ni purifications with Ni resin due to precipitation of Ca causing lowered yield of sample 4 [15]. Additionally, one laboratory reported Ni yields above 100%, which were considered acceptable due to approximately 30% uncertainty (2σ).

In total, 5 $^{3}$H and $^{14}$C results were submitted and the entries with sample numbers, sample sizes, yields and activity concentrations are presented in Table 4. All the $^{3}$H activity concentration results were above LOD and the statistical analysis was carried out by 2 iterations resulting in the $^{3}$H assigned value of 55 ± 4 Bq g$^{-1}$ (2σ). As the robust standard deviation was low (i.e. 6%), it was used in the z score calculations, which show that all the results were in acceptable range. The presented yields were also good corresponding to efficient extraction of $^{3}$H using thermal oxidation.

The $^{14}$C results in Table 4 show that only one result out of 5 data entries was above LOD and it was produced using traditional oxidative acid digestion in a closed heating mantle system. A descrepancy can be observed between samples 5 and 6 as 10 times higher amount of sample produced lower LOD than the only activity concentration result above LOD. The efficient extraction of $^{14}$C using thermal oxidation is also shown in the $^{14}$C results as in the $^{3}$H results. However, the challenges and other critical considerations are discussed later.

The analyses of $^{36}$Cl and $^{41}$Ca were optional. The submitted results are summarised in Table 5 and they show that only one result is above LOD, namely 6 ± 1 mBq g$^{-1}$. $^{36}$Cl analysis was carried out by two laboratories and the results show that sample 8 suffered from severe loss of Cl carried (i.e. 5% yield) whereas 10 g of sample 5 with high yield (93–98%) was able to produce activity concentration results above LOD.

Even though several analyses were carried out in order to submit $^{41}$Ca results (Table 5), all laboratories reported difficulties in the LSC measurement either due to spectral

**Table 4** Measured $^{3}$H and $^{14}$C activity concentrations and corresponding masses, yields and z-scores compared to measured assigned values, if applicable

| ID # | Mass (g) | $^{3}$H results | | | $^{14}$C results | |
|---|---|---|---|---|---|---|
| | | Yield (%) | Activity concentration (Bq g$^{-1}$) | z-score meas | Yield (%) | Activity concentration (mBq g$^{-1}$) |
| 5 | 0.5 | * | 51 ± 14 | 1.2 | * | 70 ± 10 |
| 6 | 5 | 90 | 53 ± 11 | 0.7 | 100 | < 40 |
| 6 | 1 | 90 | 56 ± 11 | 0.3 | 100 | < 200 |
| 8 | 1 | 76 | 58 ± 13 | 0.8 | 100 | < 2500 |
| 8 | 1 | 76 | 58 ± 13 | 0.8 | 100 | < 2500 |

*Data not submitted

**Table 5** Measured $^{36}$Cl and $^{41}$Ca activity concentrations and corresponding masses and yields

| ID # | Mass (g) | $^{36}$Cl results | | $^{41}$Ca results | |
|---|---|---|---|---|---|
| | | Yield (%) | Activity concentration (mBq g$^{-1}$) | Yield (%) | Activity concentration (mBq g$^{-1}$) |
| 5 | 10 | 93–98 | 6 ± 1 | > 93 | Spectral interference |
| 6 | 0.6 | – | – | 34 | < 300 |
| 6 | 0.6 | – | – | 24 | < 400 |
| 6 | 0.6 | – | – | 24 | < 400 |
| 6 | 1.8 | – | – | 33 | < 70 |
| 7 | 10 | – | – | 68 | < 500 |
| 8 | 2 | 5 | < 400 | – | – |

interference (sample 5), or significant quenching with white colour (samples 6–7). The spectral interference was based on an observation of an unknown signal in the LSC spectrum and it was initially hypothesised to originate from $^{45}$Ca. However, assessment of the $^{45}$Ca half-life (i.e. 163 days) and cooling time (i.e. 5 years) out ruled the hypothesis and the cause of the interference remained unknown. The colour quenching and other critical considerations in $^{41}$Ca analysis are discussed in later section. The yield for $^{41}$Ca was 24–93%, varying widely as with other determined radionuclides.

The main gamma emitters, namely $^{152}$Eu and $^{60}$Co, were optional and the results are summarised in Table 6. The efficiency calibration for sample 3 was based on experience whereas other results were calibrated as discussed earlier. The $^{152}$Eu assigned value was iterated 10 times to be $21 \pm 2$ Bq g$^{-1}$ (2σ). As the robust standard deviation of the assigned value was low (i.e. 8%), it was used in the z score calculations. The results show that only one $^{152}$Eu entry was in unacceptable range ($z \geq 3$) whereas all the other entries were in acceptable range ($z \leq 2$).

The $^{60}$Co assigned value $280 \pm 60$ mBq/g (2σ) was iterated 8 times from 7 data entries. As the robust standard deviation of the assigned value was above 20% (i.e. 24%), the uncertainty of assigned value was utilised in the z score calculations. The $^{60}$Co z score results show that three results were in warning signal range and all the others in acceptable range.

## Activation calculation results

Table 7 lists the specific activities of the activated concrete samples, which had been calculated previously using conservative assumptions on the beam tube operation [5]. As the homogeneity measurements for $^{152}$Eu showed, the measured activity concentration of 20 Bq g$^{-1}$ was significantly lower than corresponding calculated $^{152}$Eu activity concentration i.e. 480 Bq g$^{-1}$. However, nuclear waste management procedures typically use non-destructive methods (i.e. calculations in the first place) to estimate total waste volumes with conservative assumptions and eventually the waste is classified using validated nuclide vectors and measured key nuclide activity concentration. The same procedure was utilised here by scaling the calculated DTMs with measurement based assigned value of $^{152}$Eu (i.e. $21 \pm 2$ Bq g$^{-1}$),

**Table 6** Measured $^{152}$Eu and $^{60}$Co activity concentrations and corresponding masses, yields and z-scores compared to measured assigned value

| ID # | Mass (g) | $^{152}$Eu results | | $^{60}$Co results | |
|---|---|---|---|---|---|
| | | Activity concentration (Bq g$^{-1}$) | z-score meas | Activity concentration (mBq g$^{-1}$) | z-score meas |
| 1 | 20 | $21 \pm 2$ | 0.4 | $360 \pm 30$ | 2.5 |
| 2 | 2 | $26 \pm 0.3$ | 3.4 | $360 \pm 110$ | 2.5 |
| 3 | 20 | $19 \pm 1$ | 1.0 | $220 \pm 40$ | 1.9 |
| 4 | 16 | $22 \pm 4$ | 0.7 | $260 \pm 50$ | 0.6 |
| 5 | 12 | $19 \pm 2$ | 1.1 | $202 \pm 20$ | 2.5 |
| 6 | 20 | $20 \pm 0.2$ | 0.2 | $260 \pm 10$ | 0.6 |
| 7 | 18 | $20 \pm 0.3$ | 0.4 | $250 \pm 20$ | 1.0 |
| 8 | 20 | $21 \pm 2$ | 0.2 | $270 \pm 30$ | 0.3 |

**Table 7** $^{3}$H, $^{14}$C, $^{36}$Cl, $^{41}$Ca, $^{55}$Fe, $^{63}$Ni, $^{152}$Eu and $^{60}$Co activation calculation results with 2σ uncertainty

| Radionuclide | Conservative calculated activity concentration with 2σ uncertainty (mBq g$^{-1}$) | Calculated activity concentration with 2σ uncertainty (mBq g$^{-1}$) correlated with measured assigned value of $^{152}$Eu |
|---|---|---|
| $^{3}$H | $4{,}500{,}000 \pm 900{,}000$ | $200{,}000 \pm 40{,}000$ |
| $^{14}$C | $12{,}000 \pm 4400$ | $530 \pm 190$ |
| $^{36}$Cl | $530 \pm 210$ | $23 \pm 9$ |
| $^{41}$Ca | $21{,}000 \pm 5600$ | $890 \pm 240$ |
| $^{55}$Fe | $1600 \pm 400$ | $66 \pm 17$ |
| $^{63}$Ni | $7600 \pm 1800$ | $340 \pm 80$ |
| $^{152}$Eu | $480{,}000 \pm 160{,}000$ | $21{,}000 \pm 7200$ |
| $^{60}$Co | $10{,}000 \pm 2100$ | $430 \pm 90$ |

*Measured assigned value derived from participants' results

which was iterated from the participants' results (see Table 6 and corresponding text). This means a scaling factor of 21/480 = 0.0438. Another possibility would have been to choose $^{60}$Co as the key nuclide. In the second case, the scaling factor would have been 0.028, which had resulted in 36 percent difference in the final results. This indicates that there was some difference between the Co and Eu concentrations in the studied samples compared to the samples that were used to determine the original composition used in the calculation system. However, this is still minor compared to the uncertainties in the original assumptions of the neutron dose to the samples.

Additionally, the results in Table 7 show that the calculated activity concentrations decrease in order $^{3}$H > > $^{152}$Eu > $^{41}$Ca > $^{14}$C > $^{60}$Co > $^{63}$Ni > $^{55}$Fe > $^{36}$Cl even though the chemical composition of the activating elements (Table 1) decrease in order Ca > Fe > > C > N > Cl > Ni > Li > Co > Eu exhibiting significance of the thermal cross sections.

The 2σ uncertainties presented with the calculated activity concentrations were calculated using law of error propagation in multiplication. In principle, the sources of uncertainties are mass, irradiation time, reaction cross sections and neutron flux. The highest uncertainty derives from the sample composition, i.e. masses of the activating impurities. The FiR1 biological shield concrete is heterogeneous and there can be a large variation between the ratio of rocks and cement in different cores. The calculations used the measured composition, but since the studied sample was from another drill core, it may have contained slightly different rock and cement ratio and therefore an uncertainty of twenty percent was assumed. As the irradiation and decay time is based on operating diaries and therefore very well-known, an uncertainty of one month was assumed. Cross section uncertainties were estimated according to the values listed in Table 1 [29]. Due to the assumption in the reactor beam tube operations, neutron flux uncertainty is taken into account by comparing only the results correlated with measured assigned activity of $^{152}$Eu.

Comparison of the measured DTM and gamma emitter results with the $^{152}$Eu corrected calculated results in Table 7 shows varying degrees of correlation. The best correlations can be seen between the $^{152}$Eu corrected $^{60}$Co calculated result (430 ± 90 mBq g$^{-1}$) and the measured $^{60}$Co assigned value (280 ± 60 mBq g$^{-1}$) which is 65% of the calculated result. The second best correlation can be seen with the measured $^{3}$H assigned value (55 ± 4 Bq g$^{-1}$), $^{14}$C (one result, 70 ± 10 mBq g$^{-1}$) and $^{36}$Cl (one result, 6 ± 1 mBq g$^{-1}$) results with the corresponding $^{152}$Eu corrected calculated results which are approximately 28%, 13%, and 26% of the calculated values (200 ± 40 Bq g$^{-1}$, 530 ± 190 mBq g$^{-1}$, 23 ± 9 mBq g$^{-1}$, respectively). The measured $^{3}$H, $^{14}$C and $^{36}$Cl results are systematically below the calculated results. The $^{3}$H results may have been affected by diffusion of HTO within the biological shield, isotopic exchange with the atmospheric hydrogen or evaporation during sample preparation [30, 31]. Therefore, the correlation can be considered satisfactory. Also the $^{36}$Cl and $^{14}$C values can be considered satisfactory given the difficulties in measurement of stable Cl, N and C for the activation calculations of $^{36}$Cl and $^{14}$C at such low activities. Additionally, the chemical composition of the main element to produce $^{14}$C, namely N, has been given in the Table 1 as below 200 mg kg$^{-1}$ giving a conservative result in the activation calculations. As such analyses of Cl, N and C are not easy in concrete and the activation calculations may suffer from many uncertainties (see section "Activation calculation results"), which can explain the observed differences between calculated and measured.

Significant differences can be seen between the calculated and the measured $^{55}$Fe results. $^{55}$Fe results were from almost twice to over hundred times above the calculated value. The chemical analysis of stable Fe is quite straightforward process using ICP-OES as long as the element has been quantitatively released from the solid matrix. Therefore, the main reason for the deviating measured results from calculated may be the uncorrect yield correction in the measurement results as discussed before. Additionally, the $^{55}$Fe results in the activated steel [2] were also significantly different to the calculated results and one of the reasons for deviation was proposed to be the short half life (2.7 years) and unknown cooling time.

The measured $^{63}$Ni assigned value (i.e. 970 ± 380 mBq g$^{-1}$) is almost three times higher than the calculated result (i.e. 340 ± 80 mBq g$^{-1}$). This is surprising as the original Ni content in Table 1 was indicated to be below 50 mg kg$^{-1}$ and therefore, the calculated result was expected to be an overestimation rather than underestimation compared to the measured $^{63}$Ni content. One possible reason for this could be presence of interfering radionuclides, such as $^{60}$Co and $^{55}$Fe, in the $^{63}$Ni fraction. Even though no participant reported difficulties with interfering radionuclides, it is still possible that their presence has been unknown, undetermined or underestimated. Other assumptions can be linked to the presence of calcium or quenching effects in LSC due to concrete matrix which can bias the measurement of $^{63}$Ni content. Yet another possibility, which has been acknowledged earlier, is that the original stable Ni compositions in the activated and inactive concrete samples were different.

## Considerations in the activation calculations

Concrete is especially difficult material, since it is very inhomogeneous and even small variations in the ratio between rocks and cement can have a large effect if some activating impurity is mainly present in either one them. However, activity calculations provide a non-destructive first approach to estimate the volumes and activities in a decommissioning

project. Especially research reactors typically have very complicated operating history, which may also contain several structural modifications. Therefore, the calculations at the FiR1 research reactor decommissioning project also required several simplifying assumptions. These were always chosen conservatively to slightly overestimate the amount of activated waste. The assumptions on the operating history of the horizontal neutron beam tubes appeared to be slightly over conservative, which caused the large discrepancy between the calculated and measured activities. However, dismantling planning also contain other factors (e.g. mechanical and logistics) that may affect choosing the final cutting and waste management methods. Therefore, optimising the calculations for high-precision validation purposes can be very complicated.

## Critical considerations in the DTM analysis

The first critical step in the analysis of non-volatile DTMs is the quantitative release of the analytes of interest from the solid matrix. Solubility of RPV steel was not problematic as seen in the results of the first intercomparison exercise [1, 2], whereas activated concrete required harsh acid digestion treatments in order to obtain complete destruction of the solid matrix. Measurement of the chemical composition of the acid digested solution is critical for appropriate addition of carriers and subsequently yield correction and also for the determination of possible interfering stable elements (e.g. Ca and Co in Ni resin separations).

Critical considerations of $^{14}C$, $^{55}Fe$ and $^{63}Ni$ analysis were discussed by Leskinen et al. [2]. As a summary, reliable $^{14}C$ analysis requires quantitative release and conversion of carbon to $CO_2$ and trapping it into a trapping solution. In the case of acid digestion, oxidative acids are required and in the case of thermal oxidation, a catalyst and oxygen gas are needed in the $CO_2$ conversion. In thermal oxidation, the release of the analyte is also affected by temperature, which needs to follow appropriate profile based on the matrix. In addition, the yield of $^{14}C$ analysis is determined by spiking with liquid $^{14}C$ standards, as there are no commercially available reference materials. These discussions are relevant also for the $^{14}C$ analysis in activated concrete. However, due to low $^{14}C$ activity concentration of the studied activated concrete, almost all results were below LOD. Therefore, further studies with higher $^{14}C$ activity level activated concrete should be conducted. As developed in Ref. [32], the preparation of spiked in-house concretes should be investigated to determine more accurate yields for $^{14}C$ extraction from concrete pyrolysis.

The critical discussions of $^{55}Fe$ analysis by Leskinen et al. [2] can be summarised in challenges rising from the low energy decay mode of $^{55}Fe$ via electron capture e.g. (i) chemiluminescence exhibits signal in the low LSC channels similar to $^{55}Fe$, (ii) the effect of quenching is especially significant for low energy emissions, and (iii) acid tolerance of the liquid scintillation cocktails. In this study, the relatively high stable Fe content in the studied activated concrete and the difficulties in the complete destruction of the matrix caused major difficulties in the $^{55}Fe$ analysis.

The critical discussions of $^{63}Ni$ analysis by Leskinen et al. [2] focused on the importance of careful removal of $^{60}Co$ from the $^{63}Ni$ fraction. $^{60}Co$ is a prevalent interfering radionuclide in activated steel whereas it may not be as important in the studied activated concrete. In this study, no interference by $^{60}Co$ in $^{63}Ni$ fraction was reported. Most laboratories implemented a separation on an anion exchange resin in HCl medium to isolate Ni from Fe. However, as the studied sample contained high amount of Ca, the purified Ni fraction may have contained also Ca (provided that the preceding hydroxide precipitation was not performed) since both Ni and Ca are not retained on resin in concentrated HCl medium and are co-eluted [21]. The presence of high Ca amount hindered the purification of Ni on Ni resin by precipitating during the loading step of the sample and lowered the separation yield in comparison to previous works [15].

The critical considerations in $^{3}H$ analysis is similar to $^{14}C$ analysis as both of them are volatile radionuclides and pure β emitters. Analysis of this low energy pure β emitter ($E_{max} = 18.6$ keV) can be carried out using aqueous leaching, distillation, freeze-drying, azeotropic distillation, or chemical/thermal oxidative decomposition prior to LSC measurement [30]. With the exception of oxidative decomposition, quantitative analysis is subject to $^{3}H$ speciation as HTO as the above mentioned methods cannot release strongly bound $^{3}H$ [30]. For example, studies have shown that in activated concrete $^{3}H$ can be present in free water (i.e. HTO), in water of crystallisation, in structural OH-groups and be lattice bound [30]. The lattice bound $^{3}H$ originates mainly from activation of Li impurities and is the most strongly bound speciation of $^{3}H$ requiring excess of 350 °C temperatures [30, 31]. The loss of $^{3}H$ via evaporation of HTO during storage and sampling can be an issue in analysis of activated concrete. However, the loss of $^{3}H$ via evaporation can be very significant in the case of contaminated samples resulting in a negative bias in the radiochemical analysis. In thermal oxidation methods (i.e. the oxidiser and pyrolyser utilised in this study), $^{3}H$ needs to be quantitatively released from the solid matrix, converted to HTO, and trapped into a trapping solution. Therefore, the same challenges exist with $^{3}H$ as with $^{14}C$ analysis discussed by Leskinen et al. [2]. The results submitted in this study showed excellent consistency even though the analyses were carried out within a few months' time interval. As such, the storage and sending of the activated concrete samples had not caused evaporation of $^{3}H$. On the other hand, it would have been interesting to compare the thermal oxidation with acid digestion in order

to see the effectiveness of acids to liberate $^{3}H$ from mineral bound position.

$^{36}Cl$ analysis consists of extraction from matrix, its trapping and its purification prior to LSC measurement. As a volatile DTM radionuclide, $^{36}Cl$ has to be released from the matrix and trapped efficiently. The trapped $^{36}Cl$ is then isolated from the interfering radionuclides (e.g. $^{129}I$, $^{99}Tc$) and matrix elements to avoid overestimation and avoid quenching during LSC measurements. In this intercomparison, the extraction of $^{36}Cl$ from the activated concrete was carried out with acid leaching with 8 M $HNO_3$ or with combustion using a Pyrolyser. In the first case, chloride in the leachate was separated by AgCl precipitation followed by an anion exchange chromatographic purification according to Ref. [23]. The separated chloride in $NH_4Cl$ solution was then mixed with scintillation cocktail before LSC analysis. In the second case, the released chlorine was trapped in 6 mM $Na_2CO_3$ medium. Afterwards, $^{36}Cl$ was purified using AgCl precipitation and then separated from silver using anion exchange resin similarly to the first case. The combination of AgCl precipitation and anion exchange resin enabled to achieve decontamination factors higher than $10^6$ towards interfering elements such as $^{129}I$, $^{35}S$, $^{14}C$ or $^{3}H$ and to obtain accurate determination of $^{36}Cl$ in various matrices [23]. However, the implementation of AgCl precipitation and ion exchange purifications made $^{36}Cl$ analysis lengthy and can induce yield loss, especially for laboratories that do not perform this analysis routinely or are in the method development phase, as it was the case of laboratory 8 which observed a 5% yield. Another challenge of $^{36}Cl$ determination in the present intercomparison was the very low level of activity concentration. It was possible to quantify $^{36}Cl$ at a very low value of 6 mBq/g by performing a counting during 10 h and by leaching a high amount of sample (10 g). Further investigations have to be carried out to consolidate the $^{36}Cl$ determination at low level. The implementation of AMS measurements or Cl resin (by Eichrom Technologies) are options to be considered to improve the $^{36}Cl$ detection limit.

$^{41}Ca$ analysis includes at least the following features, which require critical considerations. Success in hydroxide precipitation step, where Fe and Ni are precipitated while Ca should remain in the solution, is not always complete. Instead, if pH is increased fast with saturated NaOH to basic pH values, then Ca might precipitate at lower pH and follow Fe and Ni precipitate to column separation. As discussed in "Overview of the radiochemical analyses", this decreases the yield of Ca and complicates column separation of Fe and Ni. Any interfering beta or x-ray emitting radionuclide in the final purified sample can easily ruin the LSC spectrum of $^{41}Ca$, due to extremely low energy of x-rays from $^{41}Ca$ (0.3–3.6 keV) and their equally poor intensity (strongest emission 7.8%). Although in this work the concrete matrix did not contain $^{60}Co$ at disturbing concentration level, in other cases of activated concrete $^{60}Co$ can be present in higher amounts. In that case, $^{60}Co$ should be removed carefully from the $^{41}Ca$ fraction by several repeating precipitations and monitoring the decontamination progress by gamma measurements of the purified fractions [17]. Last critical step is dissolution of the evaporation residue containing $^{41}Ca$, either to HCl or to $H_2O$ prior to adding scintillation cocktail. Regardless of the used solvent, the produced LSC sample should be clear, without white or other colour precipitate. Chemical quenching is particularly destructive for $^{41}Ca$ samples, combined to fore mentioned low energy and intensity of $^{41}Ca$ x-rays it leads to incredibly low counting efficiency. For example, sample 7 in this study gave only 2% counting efficiency due to these three factors together. For standard samples (with no quenching), a higher but still low efficiency value of 7% was obtained, representing the best possible counting efficiency for $^{41}Ca$ with this setup. Therefore, it is essential to eliminate colour quenching from an LSC sample of $^{41}Ca$.

## Critical considerations in the gamma emitter analysis

Critical considerations of $^{60}Co$ analysis have been discussed by Leskinen et al. [2]. As a summary, reliable gamma emitter analysis requires properly maintained and calibrated detector, suitable measurement geometry for the sample size and activity level and coincidence correction especially with short source-to-detector distance. Additionally, the most reliable efficiency calibration is possible using experimental measurements with reference material as close as possible to sample matrix [33]. However, the analysis of $^{152}Eu$ is more complicated compared to $^{60}Co$, since $^{152}Eu$ decays with electron capture, positron emission and $\beta-$ sending out X-rays (4 photons), betas and gammas (132 photons). As such $^{152}Eu$ has a wide range of peaks which can result in significant true coincidence summing (TCS). The true coincidence summing occurs also in the case of $^{60}Co$ decaying by emission in cascade 1173 and 1333 keV gamma rays. The size of TCS factor depends on the measurement geometry, the decay scheme and detector dimensions. Correction factor of 0.91–1.57 for different energies of $^{152}Eu$ has been published in Ref. [34]. In this intercomparison at VTT, correction factors of 0.96–1.22 for different energies of $^{152}Eu$ were used. In addition to TCS, coincidence summing can also be random coincidence, in which different nuclei emit radiations (x-rays, annihilation photons and gammas) that are close in time compared to the detector response time [35]. This phenomenon is more probable at higher activities and as such, the phenomenon was not significant in this study, because the samples contained low activities. As a conclusion, if coincidence is not corrected for, the activity determination of a sample can be significantly underestimated. Therefore,

coincidence summing is a common source of systematic errors in gamma spectrometry.

### Critical considerations on uncertainty calculations

Uncertainty calculations were further performed as recommended by Leskinen et al. [2] and the laboratories were requested to submit further details in their uncertainty calculations. Majority of the provided uncertainties were evaluated according to GUM method [36]. The calculations were based on the combination of the different sources of uncertainties. They included measurement uncertainties (e.g. LSC and yield measurements), uncertainties in the radiochemical analysis (e.g. weights, volumes, standards, etc.) and uncertainties in the digestion step. It can be underlined that one laboratory assumed a 10% uncertainty at 2σ for the digestion step based on the results obtained on inactive muds during intercomparison exercises. For one laboratory, only the counting uncertainty was considered. One laboratory also applied the Kragten numerical method [37]. Very different values of uncertainties were calculated: for example, for $^{55}$Fe, the uncertainties varied from 2.4% up to 160%. Therefore, it can be noticed that the uncertainty calculations differed from one laboratory to another. The estimation of source uncertainties is not an easy task to complete. However, the major source of uncertainty was determined to originate from activity measurement by LSC (measurement statistics and efficiency curve) whatever the applied method because the activity concentrations were very low. The other important uncertainties in LSC are due to low energies, quenching difference related to the difference in chemical compositions of standard used for calibration and sample, the implementation of TDCR method with HIDEX 300SL device, the background as well as the scintillator type. Further studies should be carried out in order to take into account all sources of uncertainties and consolidate their estimations. The next intercomparison should help to improve the uncertainty evaluation and to harmonise the practices between laboratories.

### Critical considerations on limit of detection calculations

The LODs of participating laboratories for $^{55}$Fe, $^{63}$Ni, $^{41}$Ca and $^{14}$C were < 300–< 500, < 90–< 600, < 70–< 500 and < 40–< 2500 mBq/g, respectively. The LODs for $^{55}$Fe and $^{63}$Ni are well below the exemption limits or clearance of materials stated in 2013/59/Euratom directive, namely 1000 Bq/g for $^{55}$Fe and 100 Bq/g for $^{63}$Ni [38]. For $^{41}$Ca, there is no exemption limit, due to weak energy and intensity of the x-ray emissions. For $^{14}$C, the corresponding exemption limit or clearance of materials is 1 Bq/g, which means that part of the calculated LODs are higher than the exemption limit, although the LODs and exemption limit for $^{14}$C are at the same concentration level. On the other hand, maximum LOD value of 2.5 Bq/g is still very far from exemption value for the activity concentration of $^{14}$C in moderate amounts of any type of material, which is 10 000 Bq/g [38]. Nevertheless, disposal of materials which activity concentrations are below LOD needs still careful attention and comparison of LODs against exemption limits, as this example points out. The combination of relatively high LOD with relatively low exemption limit increases the need for optimising radioanalytical separation methods and measurement techniques for decreasing LOD (e.g. longer measurement time), as well as reassessing the calculation method for LOD.

As the studied activated concrete contained low levels of radioactivities, results below LOD were expected. This initiated discussion on how the laboratories calculated their LOD and it was found out that several different calculation methods were used among participating laboratories. Currie's classical method [39], ISO 11,929–1:2019 standard method [40], French standards NF M60-322 and NF M60-317 [41, 42] have been used for calculating LODs in this work, as well as a simple approach using the value 3 times of the blank uncertainty in consideration of counting efficiency and chemical recovery. It can be seen throughout the reported results, that the LOD values have wide variation among laboratories, often 100-fold. Because laboratories use firstly different radioanalytical separation methods, and different measurement methods and instruments and furthermore, use different calculation methods for producing LODs, comparison of obtained results is sometimes difficult and the range for LOD values is therefore broad. These considerations suggest that in the forthcoming intercomparison projects, emphasis should be given to more uniform practices for calculating, not only LODs, but also uncertainties. In general, harmonised and ambiguous calculation methods should be taken into use, for facilitating comparison of results from different laboratories.

## Conclusions

The second year of intercomparison exercise on DTM analysis in decommissioning waste can be concluded similarly to the first year, that the analysis of beta-emitter radionuclides in decommissioning waste is difficult especially at very low level. No major difficulty was observed for the $^{3}$H analysis as the analysis was carried out using thermal oxidation and the measured results were in good agreement. In addition, the possible volatility of $^{3}$H during the project was not observed to cause a bias in the measured results. However, comparison of the measured $^{3}$H results ($55 \pm 4$ Bq g$^{-1}$) with calculated activity concentration ($200 \pm 40$ Bq g$^{-1}$) showed that loss of $^{3}$H during sampling, storage and drilling may

have occurred. Additionally, migration of $^{3}H$ within the biological shield could have affected the results. Low activity level caused difficulties in the $^{14}C$ analysis, as the thermal oxidation was not able to produce results above LOD even though it is a well-established technique. One laboratory was able to produce a $^{14}C$ activity concentration result, which was relatively well correlated with the calculated result (i.e. $70 \pm 10$ mBq $g^{-1}$ versus $530 \pm 190$ mBq $g^{-1}$) considering the uncertainties in the original chemical composition of nitrogen. Analysis of $^{36}Cl$ was carried out by two laboratories; one well advanced in the $^{36}Cl$ analysis and another in process of $^{36}Cl$ method development. A significant difference between the yields was observed i.e. 5% and over 93%. The only $^{36}Cl$ activity concentration result above LOD correlated well with the corresponding calculated result (i.e. $6 \pm 1$ mBq $g^{-1}$ versus $23 \pm 9$ mBq $g^{-1}$). Major difficulties were observed in the $^{41}Ca$ analysis as the relatively easy purification method via precipitations resulted in spectral interferences in LSC measurements due to possible presence of an interfering radionuclide or severe quenching. Also, major difficulties were observed in the $^{55}Fe$ analysis. The comparison of the measured $^{55}Fe$ activity concentration results above LOD with the corresponding calculated results showed unacceptable differences ranging from almost 200% up to 13,500% higher measured results most likely due to difficulties in the yield corrections and also due to short half-life. The analysis of $^{63}Ni$ was a quite straightforward process, as no interfering gamma emitters were observed in the purified fractions. On the other hand, low $^{63}Ni$ activity concentration caused majority of the submitted results to be below LOD. Comparison of the measured $^{63}Ni$ assigned value with the corresponding calculated result (i.e. $970 \pm 380$ mBq $g^{-1}$ versus $320 \pm 80$ mBq $g^{-1}$) showed measured values to be approximately three times higher, possibly due to overestimated amount of $^{63}Ni$ due to spectral interference in $^{63}Ni$ determination or different original stable Ni composition in the studied activated samples and inactive sample, from which the activation calculations were derived.

As a conclusion, the second year of the intercomparison exercise project further strengthened the radiochemical methods for DTM analysis and the participating laboratories benefitted from the analyses and discussions. The calculation results also underlined the importance of the input data i.e. in this case the chemical composition and irradiation history. The calculated results in activated concrete were not as well aligned with the measured results as in activated steel, because the input data had higher uncertainties. However, the calculated results in this paper are in a sense more realistic as majority of the materials in decommissioning projects suffer from conservative assumptions in the activation calculations.

The third year of intercomparison exercise will be on DTM analysis in spent ion exchange resin. As such, the analyses will be carried out for DTMs originating from both the spent fuel (e.g. $^{90}Sr$) and corrosion products (e.g. $^{55}Fe$ and $^{63}Ni$).

**Acknowledgements** The authors would like to thank the Nordic Nuclear Research NKS-B programme (www.nks.org) for funding the DTM Decom project in which the intercomparison exercise was carried out. The authors would also like to thank the other participating laboratories, namely Technical University of Denmark, Cyclife Sweden AB, Fortum Power and Heat Oy, IFE Kjeller and IFE Halden for provision of data and collaboration. National fundings were given by Finnish Research Programme on Nuclear Waste Management KYT 2022. A-LABOS-EX-PR-SC-01 project is thanked for the CEA self-funding. The authors would also like to thank FiR1 decommissioning personnel for the provision of studied material and collaboration.

**Funding** Open access funding provided by Technical Research Centre of Finland (VTT).



## References

1. Leskinen A, Tanhua-Tyrkkö M, Kekki T, Salminen Paatero S, Zhang W, Hou X, Stenberg Bruzell F, Suutari T, Kangas S, Rautio S, Wendel C, Bourgeaux-Goget M, Stordal S, Isdahl I, Fichet P, Gautier C, Brennetot R, Lambrot G, Laporte E (2020). Intercomparison exercise in analysis of DTM in decommissioning waste. NKS-429, NKS-B, Roskilde, Denmark. ISBN 978-87-7893-519-9
2. Leskinen A, Salminen Paatero S, Gautier C, Räty A, Tanhua-Tyrkkö M, Fichet P, Kekki T, Zhang W, Bubendorff J, Laporte E, Lambrot G, Brennetot R (2020) Intercomparison exercise on difficult to measure radionuclides in activated steel: statistical analysis of radioanalytical results and activation calculations. J Radioanal Nucl Chem 324:1303–1316
3. International Standard ISO 13528:2015(E) (2015) Statistical methods for use in proficiency testing by interlaboratory comparison. ISO, Geneva
4. Leskinen A, Tanhua-Tyrkkö M, Salminen Paatero S, Laurila J, Kurhela K, Hou X, Stenberg Bruzell F, Suutari T, Kangas S, Rautio S, Wendel C, Bourgeaux-Goget M, Moussa J, Stordal S, Isdahl I, Gautier C, Laporte E, Guiliani M, Bubendorff J, Fichet P (2021). DTM-Decom II - Intercomparison exercise in analysis of DTM in decommissioning waste. NKS-441, NKS-B, Roskilde, Denmark. ISBN: 978-87-7893-533-5
5. Kotiluoto P, Räty A (2016) FiR 1 activity inventories for decommissioning planning. VTT Research report series, VTT-R-03599–16

6. Gauld IC, Radulescu G, Ilas G, Murphy BD, Williams ML (2011) Isotopic depletion and decay methods and analysis capabilities in scale. Nucl Technol 174:169–195
7. Räty A, Kekki T, Tanhua-Tyrkkö M, Lavonen T, Myllykylä E (2018) Preliminary waste characterization measurements in FiR 1 TRIGA research reactor decommissioning project. Nucl Technol 203(2):205–220
8. Räty A, Lavonen T, Leskinen A, Likonen J, Postolache C, Fugaru V, Bubueanu G, Lungu C, Bucsa A (2019) Characterization measurements of fluental and graphite in FiR1 TRIGA research reactor decommissioning waste. Nucl Eng Design 353:110198
9. Räty A (2020) Activity characterisation studies in FiR1 TRIGA research reactor decommissioning project, Doctoral school in natural sciences dissertation series, URN:ISSN:2670–2010
10. X-5 Monte Carlo Team (2003) MCNP – A General Monte Carlo N-Particle transport code, Version 5, Los Alamos National Laboratory, LA-UR-03–1987
11. Räty A, Kotiluoto P (2016) FiR 1 TRIGA activity inventories for decommissioning planning. Nucl Technol 194:28–38
12. Beckurts KH, Wirtz K (1964) Neutron physics, appendix I 407–416. Springer-Verlag, Berlin Heidelberg
13. Leskinen A, Salminen-Paatero S, Räty A, Tanhua-Tyrkkö M, Iso-Markku T, Puukko E (2020) Determination of $^{14}$C, $^{55}$Fe, $^{63}$Ni and gamma emitters in activated RPV steel samples: a comparison between calculations and experimental analysis. J Radioanal Nucl Chem 323:399–413
14. Gautier C, Laporte E, Lambrot G, Giuliani M, Colin C, Bubendorff J, Crozet M, Mougel C (2020) Accurate measurement of $^{55}$Fe in radioactive waste. J Radioanal Nucl Chem 326:591–601
15. Gautier C, Colin C, Garcia C (2015) A comparative study using liquid scintillation counting to determine $^{63}$Ni in low and intermediate level radioactive waste. J Radioanal Nucl Chem 308:261–270
16. Eichrom Method (2014) Nickel-63/59 in water, No NIW01 analytical procedure revision 1.3. https://www.eichrom.com/wp-content/uploads/2018/02/niw01-13_ni-water.pdf
17. Ervanne H, Hakanen M, Lehto J, Kvarnström R, Eurajoki T (2009) Determination of 45Ca and γ-emitting radionuclides in concrete from a nuclear power plant. Radiochim Acta 97:631–636
18. Hou X (2005) Rapid analysis of $^{14}$C and $^{3}$H in graphite and concrete for decommissioning of nuclear reactor. Appl Radiat Isotop 62:871–882
19. Hou XL (2005) Radiochemical determination of $^{41}$Ca in reactor concrete for decommissioning. Radiochim Acta 93:611–617
20. Hou X. (2018) Analytical procedure for simultaneous determination of $^{63}$Ni and $^{55}$Fe. NKS-B RadWorkshop
21. Hou X, Østergaard LF, Nielsen SP (2005) Determination of $^{63}$Ni and $^{55}$Fe in nuclear waste samples using radiochemical separation and liquid scintillation counting. Anal Chim Acta 535(1–2):297–307
22. Hou XL, Østergaard LF, Nielsen SP (2005) Determination of $^{63}$Ni and $^{55}$Fe in nuclear waste and environmental samples. Anal Chim Acta 535:297–307
23. Hou XL, Østergaard LF, Nielsen SP (2007) Determination of $^{36}$Cl in nuclear waste from reactor decommissioning. Anal Chem 79:3126–3134
24. Itoh M, Watanabe K, Hatakeyama M, Tachibana M (2002) Determination of $^{41}$Ca in biological-shield concrete by low-energy X-ray spectrometry. Anal Bioanal Chem 372:532–536
25. Nottoli E, Bourles D, Bienvenu P, Labet A, Arnold M, Bertaux M (2013) Accurate determination of $^{41}$Ca concentrations in spent resins from the nuclear industry by accelerator Mass spectrometry. Appl Rad Isot 82:340–346
26. Triskem International (2013) Cl-36/I-129 separation, analytical method TKI-CL-01 version 1.4. https://www.triskem-international.com/scripts/files/5b1e843fd6f687.29547776/tki_cl01_v-14_en_1--1.pdf
27. Kojima S, Furukawa M (1985) Liquid Scintillation Counting of $^{55}$Fe Applied to Air-filter Samples. Radioisot 34:72–77
28. Priya S, Gopalakrishnan RK, Goswami A (2014) TDCR measurements of 3H, 63Ni and 55Fe using Hidex 300SL LSC device. J Radioanal Nucl Chem 302:353–359
29. NRG Petten, nuclear reaction program TALYS, http://www.talys.eu/home/ (accessed on 5.8.2019)
30. Kim JK, Warwick PE, Croudace IW (2008) Tritium speciation in nuclear reactor bioshield concrete and its impact on accurate analysis. Anal Chem 80:5476–5480
31. Warwick PE, Kim D, Croudace IW, Oh J (2010) Effective desorption of tritium from diverse solid matrices and its application to routine analysis of decommissioning materials. Anal Chim Acta 676:93–102
32. Brennetot R, Giuliani M, Guégan S, Fichet P, Chiri L, Deloffre P, Masset A, Mougel C, Bachelet F (2017) $^{3}$H measurement in radioactive wastes: efficiency of the pyrolysis method to extract tritium from aqueous effluent, oil and concrete. Fusion Sci Technol 71:397–402
33. Harms A, Gilligan C (2010) Development of a neutron-activated concrete powder reference material. Appl Rad Isot 68:1471–1476
34. Rodenas J, Gallardo S, Ortiz J (2007) Comparison of a laboratory spectrum of $^{152}$Eu with results of simulation using the MCNP code. Nucl Instrum Methods A 580:303–305
35. Shweikani R, Hasan M, Takeyeddin M (2013) A simplified techniques to determine random coincidence summing of gamma rays and dead time count loss corrections. Appl Radiat Isotop 82:72–74
36. Joint Committee for Guides in Metrology (2008) Evaluation of measurement data - Guide to the expression of Uncertainty in Measurement, JCGM 100:2008, 2nd ed.
37. Kragten J (1994) Calculating standard deviations and confidence intervals with a universally applicable spreadsheet technique. Analyst 119:2161–2165
38. 2013/59/Euratom directive. https://eur-lex.europa.eu/legal-content/EN/TXT/?uri=CELEX%3A32013L0059
39. Currie LA (1968) Limits for qualitative detection and quantitative determination. Application to radiochemistry. Anal Chem 40(3):586–593
40. International Standard ISO 11929-1:2019 (2019) Determination of the characteristic limits (decision threshold, detection limit and limits of the coverage interval) for measurements of ionizing radiation – Fundamentals and application – Part 1: Elementary applications
41. NF M60–322 (2005) Technologie du cycle du combustible nucléaire – Déchets – Détermination de l'activité du fer 55 dans les effluents et déchets par scintillation liquide, après séparation chimique préalable. Association Française de Normalisation, Paris, France.
42. NF M60–317 (2001) Technologie du cycle du combustible – Déchets – Détermination de l'activité du nickel 63 dans les effluents et déchets par scintillation liquide, après séparation chimique préalable. Association Française de Normalisation, Paris, France.